Electron Transfer in Proton–Hydrogen-Atom Collisions: 2–117 keV*

G. W. McClure
Sandia Laboratory, Albuquerque, New Mexico
(Received 11 March 1966)

The cross section for electron transfer between a proton and a hydrogen atom has been measured in the energy range 2 to 117 keV. The apparatus employs a heated target chamber in which hydrogen gas is 79% dissociated. The total density of H atoms in the collision chamber, including both free H atoms and H atoms combined into H_2 molecules, is determined by a differential-Coulomb-scattering measurement, while the density of H_2 molecules is determined by a double-electron-capture measurement. Experimental values of the cross section measured at 19 different energies varied monotonically from 13.3×10^{-16} cm^2 at 1.92 keV to 0.064×10^{-16} cm^2 at 117.5 keV. The results, believed to be accurate to $\pm5\%$, are not completely consistent with previous measured values of other investigators. Theoretical calculations of McCarroll and McElroy agree satisfactorily with the measurements at energies lower than 60 keV, but between 60 and 117 keV no theoretical calculation is in satisfactory agreement with the measurements.

I. INTRODUCTION

THE transfer of an electron from an H atom to a proton, represented by the reaction equation,

$$H^+ + H \rightarrow H + H^+ \quad \text{(reaction I)},$$

has been studied by several theoretical approaches.[1–8] It is one of the simplest atomic collisions to handle theoretically because only one electron is involved. Several experimental investigations[9–12] have given cross-section values over the energy range 20 eV to 138 keV, but the experimental uncertainties vary from 10 to 30%. It is highly desirable to reduce the experimental uncertainties by a factor of 2 or 3 and thereby provide a more stringent test of the relative merits of the various theories which differ in their predictions by 20 to 50% in the 1- to 100-keV range.

This paper reports new cross-section measurements in the 2–117-keV energy range performed by a method yielding the desired improved precision. The apparatus comprises an atomic-hydrogen target similar to that used by Lockwood[13] and Helbig[14] in studies of charge transfer in violent proton–H-atom collisions. In this type of apparatus the density of H atoms in the collision chamber is much higher than the density of background gas molecules. This desirable condition was not achieved in the above referenced total-cross-section measurements wherein a relatively low-density H-atom beam emergent from a furnace was used as a target. In the present measurement there was no need to work with chopped beams and phase-sensitive particle detectors as was done in all of the previous total-cross-section measurements. Methods developed by Lockwood and co-workers[15] were employed to determine the target thickness and to compensate for the residual undissociated H_2 gas in the target chamber.

The present method registers the occurrence of reaction I by detecting the fast H atoms emergent from the collision chamber. In this respect the measurement is similar to that of Ryding and Gilbody[12] but dissimilar to that of Fite and co-workers[10,11] who utilized the algebraic sum of the slow electron and slow positive ion currents generated in the beam crossing region as a measure of the charge transfer process.

The method entails a determination of the ratio σ_1/σ_2, where σ_1 is the cross section for reaction I and σ_2 is the cross section for the reaction

$$H^+ + H_2 \rightarrow H + H_2^+. \quad \text{(reaction II)}$$

The value of σ_1 is determined by independent measurements of σ_1/σ_2 and σ_2 to within 3%. The absolute determination of σ_2 is done via subsidiary measurements of the Coulomb scattering of protons in the gas target for which accurate and simple theory exists for calculation of the cross section.[15]

Total-cross-section measurements of the present type augment the detailed experimental work of Lockwood and co-workers[13] and Helbig and co-workers[14] on the probability of proton–H-atom charge exchange in

* This work was supported by the U. S. Atomic Energy Commission.

[1] Theoretical work prior to 1962 has been reviewed by D. R. Bates, *Pure and Applied Physics 13, Atomic and Molecular Processes* (Academic Press Inc., New York, 1962), p. 550.

[2] M. B. McElroy, Proc. Roy. Soc. (London) **A272**, 542 (1963).

[3] I. M. Cheshire, Proc. Phys. Soc. (London) **82**, 113 (1963).

[4] I. M. Cheshire, Proc. Phys. Soc. (London) **84**, 89 (1964).

[5] S. E. Lovell and M. B. McElroy, Proc. Roy. Soc. (London) **A282**, 100 (1964).

[6] L. Wilets and D. F. Gallaher, in *Abstracts of the Fourth International Conference on the Physics of Electronic and Atomic Collisions, Quebec, 1965* (Science Bookcrafters, Hastings-on-Hudson, New York, 1965), p. 340.

[7] J. Grant and J. Shapiro, Proc. Phys. Soc. (London) **86**, 1007 (1965).

[8] J. M. Peek, Phys. Rev. **143**, 33 (1966).

[9] W. L. Fite, R. T. Brackmann, and W. R. Snow, Phys. Rev. **112**, 1161 (1958).

[10] W. L. Fite, R. F. Stebbings, D. G. Hummer, and R. T. Brackmann, Phys. Rev. **119**, 663 (1960).

[11] W. L. Fite, A. C. H. Smith, and R. F. Stebbings, Proc. Roy. Soc. (London) **A268**, 527 (1962).

[12] G. Ryding and H. B. Gilbody, in *Abstracts of the Fourth International Conference on the Physics of Electronic and Atomic Collisions, Quebec, 1965* (Science Bookcrafters, Hastings-on-Hudson, New York, 1965), p. 302. Data shown in Fig. 4 were communicated privately in advance of publication.

[13] G. J. Lockwood and E. Everhart, Phys. Rev. **125**, 567 (1962).

[14] H. F. Helbig and E. Everhart, Phys. Rev. **136**, 674 (1964).

[15] G. J. Lockwood, H. F. Helbig, and E. Everhart, J. Chem. Phys. **41**, 3820 (1964).

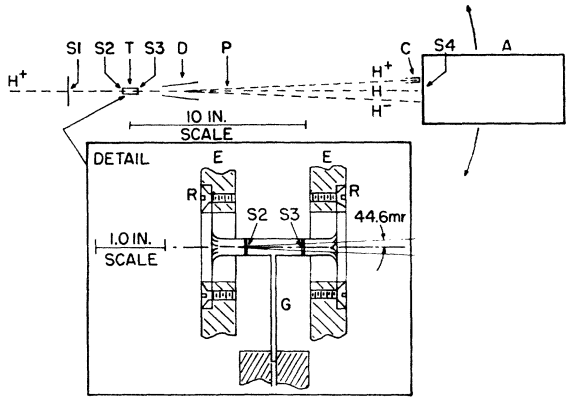

FIG. 1. Apparatus. A monoenergetic proton beam entering from the left is collimated by apertures S1 (0.020 in. diam) and S2 (0.010 in. diam). Collision chamber T, with structural details shown in the insert, has gas inlet G and exit aperture S3 (0.080 in. diam). Deflection plates D divide beam emergent from T into H^+ H, and H^- components. Beams H^+ and H^- are typically deflected ± 53 mrad from the H beam. Faraday cup C receives H^+ primary particle beam, and proportional counter A detects H and H^- secondary particle beams. Entrance aperture S4 to counter A is 0.001 in. wide in direction parallel to plane of figure and 0.963 in. wide in direction perpendicular to plane of figure. Arrows indicate direction of motion of A about center P permitting stepwise scanning of the H and H^- beams to determine their intensities. The walls of T are made of 0.001-in. tungsten foil rolled into two layers and heated by conduction of electric current applied at terminals E through clamps R. The sequence of components S1 through D is mounted on gimbals to permit precise alignment with the H^+ beam. All parts shown, except the interior of counter A and the interior of collision chamber T, are located in a 4-in.-diam cylindrical high-vacuum vessel pumped by two 400-liter/sec oil diffusion pumps.

large-angle collisions. The large-angle measurements with well-defined angles are of great theoretical interest, since the scattering angle identifies the impact parameter.

The apparatus and experimental method are described in Sec. II. The equations used in deriving cross sections from measured quantities are discussed in Sec. III. The results of electron-transfer cross-section measurements of H^+ in H gas and H^+ in H_2 gas and the relationship between the present and previous experimental results are discussed in Sec. IV. The present results for H^+ charge transfer in H gas are compared with theoretical calculations in Sec. IV.

II. APPARATUS

The portion of the apparatus specially developed for this measurement is shown in Fig. 1. Details of the proton accelerator and magnetic analyzer located to the left of the apparatus segment shown in Fig. 1 have been given previously.[16] The beam entering collimation slit S1 had an energy spread of less than 1%. This beam was passed into a collision chamber T into which hydrogen gas was admitted at a measured flow rate. The gas in the chamber was either pure molecular hydrogen or a mixture of molecular and atomic hydrogen depending on the chamber-wall temperature. Dissociation occurred as a result of catalytic interaction of the H_2 with the chamber wall of heated tungsten.[15]

In traversing the target gas within the collision chamber the proton beam underwent reactions I and II and the additional reaction[17]

$$H^+ + H_2 \rightarrow H^- + 2H^+. \quad \text{(reaction III)}$$

The yield of fast H^- ions from reaction III was employed as a direct indication of the relative density of H_2 gas in the chamber as a function of gas flow rate and wall temperature.

The composite beam emergent from the collision chamber exit aperture consisted of H^+, H, and H^- particles proceeding predominantly within an angle of a few milliradians of the direction of the incident beam and having essentially the same velocity as the incident beam. The composite beam was separated into its three components by means of electrostatic deflection plates D so that the particle current of each component could be measured separately.

The detector of the H and H^- beams was a proportional counter A having a narrow slit aperture S4 covered by a thin collodion film.[16] The window served as a gas barrier between the high-vacuum region where the deflection plates were located and the relatively high-pressure ionization region inside the counter. In the energy range of this study the counter responded to each particle entering the slit aperture with at least 99% efficiency and produced an electrical impulse clearly distinguishable from system noise. H^+, H, and H^- particles of the same velocity produced identical pulse-height distributions. The maximum detector count rate used in these measurements was 10^4 counts/sec for which the dead-time counting loss was less than 1%.

Since the aperture S4 was narrow compared to the H and H^- particle beams to be measured, only a small fraction of either beam was intercepted with a fixed slit position. The total yield of each species was therefore determined by stepwise scanning of the slit across each of the three components of the beam. This was accomplished with the aid of a proton beam current integrator attached to cup C and a mechanical counter drive. These were arranged so that the counter slit advanced a specified distance for a preset quantity of proton charge collected in cup C. During each beam scan a scaler recorded the total count summed over all slit positions and a recorder plotted the beam profile.

The results of typical scans across the H and H^- secondary beams are shown in Fig. 2. These results demonstrate the strong forward directionality of the collision products. The central peaks are 1 to 3 mrad wide and are much narrower than either the 58-mrad angle subtended by the detector slit vertical dimension

[16] G. W. McClure, Phys. Rev. 130, 1852 (1963).

[17] G. W. McClure, Phys. Rev. 132, 1636 (1963).

or the 89-mrad angle subtended by aperture S3 from aperture S2. The beam patterns obtained with the collision chamber at a higher temperature were broader than those obtained with a low temperature because of magnetic fields produced by the 60-cps collision-chamber heating current.

The proton beam emergent from S3 was received by Faraday cup C whose entrance aperture of 0.250-in. diam intercepted the entire beam. The return of secondary electrons produced by beam impingement in the cup and the rejection of electrons from sources outside the cup was accomplished by the use of a 60-V negatively biased metal ring around the entrance aperture of the cup. The photoelectric emission from the biased ring due to the incandescent collision chamber proved to be insignificant in comparison to the proton beam current. On the basis of these considerations it was believed that the cup registered the true proton beam current. Typically the beam current received in cup C was 10^{-13} A.

The tungsten chamber T was electrically heated by direct passage of an ac current through its walls. During the experiment the chamber was operated at two standard temperatures, 2373 and 295°K. The upper temperature was reached with an oven current of 144 A rms and was determined by means of an optical pyrometer. The lower temperature was reached with the heating power turned off and was measured by means of a thermometer on flange E. The upper temperature was maintained constant within 50°K and the lower temperature was maintained within 1°K.

The hydrogen gas used in the collision chamber was purified by diffusion through the 0.020-in.-thick wall of nickel tube in the gas feed line.[18,19] This tube was heated by direct passage of an electrical current through its wall. Manual control of the flow to a precision greater than 1% was maintained during the data runs by adjustment of the nickel leak heating power. The flow of gas into the collision chamber was measured by means of a diaphragm-type differential pressure gauge.[20] This gauge indicated the pressure drop created by the gas flow along a short section of small-diameter gas line between the nickel leak and the gas feed tube G leading into the chamber. Two standard flow rates were employed corresponding to pressure differentials across the small-diameter gas line section of 1 and 129 μ of Hg. The higher flow gave a calculated gas pressure of 0.5×10^{-3} mm Hg in the collision chamber at 295°K. The furnace gas density corresponding to a fixed flow rate decreased about a factor of 3 when the furnace was heated because of the higher velocity of the molecules and atoms in the furnace at higher temperatures.

Attenuation of the proton beam due to charge-exchange collisions in the collision chamber attained a maximum value of 1.7% at the higher flow rate and lower temperature and 0.6% at the higher flow rate and higher temperature. This attenuation was easily determined by comparing the yield of fast charge-exchange products H and H^- with the proton beam intensity. Beam attenuation was ignored in the data reduction since the error involved was at most 0.8% and was small compared to other experimental uncertainties.

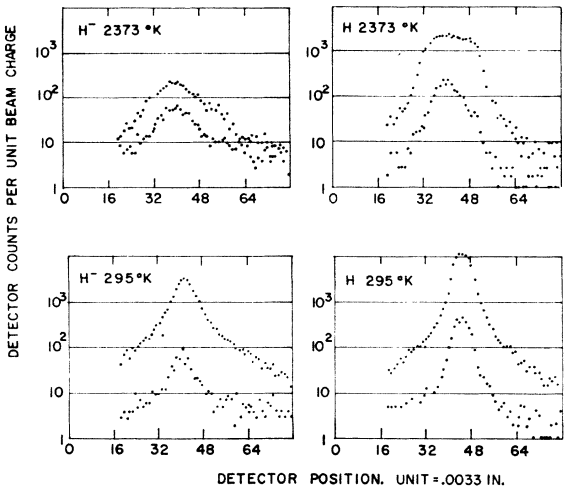

FIG. 2. Detector counts per unit proton charge collected in cup C versus horizontal position of detector slit S4. Results are shown for H^- and H beams at upper and lower standard collision-chamber temperatures, 2373 and 295°K, and at two standard gas flow rates. The upper and lower sets of points in each section of the figure correspond to the higher and lower standard flow rates. These results were obtained at a proton beam energy of 20 keV. Broadening at high temperature is explained in the text. Graphs corresponding to the lower flow rate show the maximum contribution from H and H^- production in residual gases ahead of deflection plates D and at edges of collimation slits S1 and S2.

The space surrounding furnace T was pumped by an oil diffusion pump having an estimated conductance of 1500 liter/sec for H_2 gas at 295°K. The combined conductance of apertures S2 and S3 at the same temperature was ~1.5 liter/sec so that the partial pressure of H_2 in the beam drift spaces upstream and downstream from T was $\sim10^{-3}$ times that in the furnace. The residual drift space pressure reached a maximum of 0.5×10^{-6} mm Hg when the oven power was fully on and the gas flow was set at the higher standard value. Attenuation of all beams (H^+, H, and H^-) in the gases downstream from T was less than 0.14% and could be ignored. Conversion of H^+ to H in residual gases ahead of T produced a residual component of H atoms in the proton beam entering S2 which was usually less than 3% of the H production in the furnace at the higher flow rate.

During the Coulomb-scattering measurements, which were carried out only at 20 keV, the deflection voltage on plate D was reduced to zero and Faraday cup C was moved to a point directly in line with the undeflected proton beam. Measurements of the Coulomb-scattered yield of H^+, H, and H^- (which, taken together, in-

[18] K. Landecker and A. Gray, Rev. Sci. Instr. **25**, 1151 (1954).
[19] E. R. Harrison and J. C. Hobbs, Rev. Sci. Instr. **27**, 332 (1956).
[20] M. K. S. Instruments, Inc., Model 77H-10.

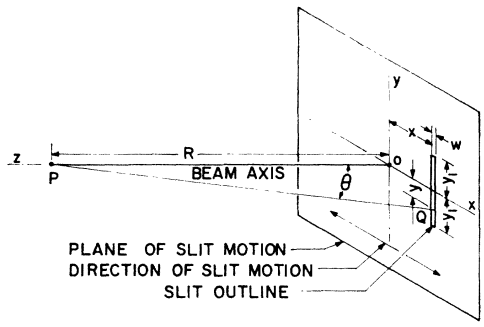

FIG. 3. Slit geometry diagram showing definition of quantities used in cross-section derivations. Point P represents the center of the collision chamber. Since R is large compared to x and y, angle $\theta \simeq (x^2+y^2)^{1/2}/R$. This approximation was substituted in Eq. (3) when the integration [Eq. (2)] was performed over the slit area to find σ_c.

cluded all final charge states of the projectile ions) were then made with the detector slit placed at fixed positions of ± 14.0 mrad relative to the proton beam center. At these positions no blockage of scattered particles by the cup or the edge of slit S3 occurred. Because of the extreme sensitivity of the Coulomb-scattered intensity to scattering angle, the scattered intensities were measured at both the $+14$ and -14 milliradian angles and were checked for equality to ensure that the beam center was correctly located.

III. CROSS-SECTION DETERMINATION

Determinations of σ_2 were made at the lower standard oven temperature under which the hydrogen gas within the collision chamber was entirely in the molecular state. Cross-section values were calculated from the formula

$$\sigma_2(E)=\sigma_c(E_c,x_c)\frac{x_1}{w}\frac{N_0(T_a,E)}{n_c(T_a,E_c,x_c)}, \tag{1}$$

where σ_c= the theoretical cross section for Coulomb scattering into the slit; N_0= the difference between the measured total H-atom yields determined by beam scans at the two standard flow rates, normalized to a standard unit of proton charge collected in cup C at each slit position during the scan and normalized to a standard displacement between successive slit positions; n_c= the difference between the total Coulomb-scattered counts of H, H^+, and H^- determined at the higher and lower standard flow rates normalized to a standard unit of proton charge collected in cup C; w= the counter slit width; x_1= the standard slit displacement used as the basis of the normalization of N_0; x_c= slit position used in the measurement of n_c; E= kinetic energy of the incident protons for the measurement of N_0; E_c= kinetic energy of the incident protons for the measurement of n_c; and T_a= the lower standard collision-chamber temperature.

The meaning of the various geometrical quantities appearing in the above discussion and in the discussion to follow is clarified in Fig. 3.

The cross section $\sigma_c(E_c,x_c)$ was calculated from the formula

$$\sigma_c(E_c,x_c)=\frac{w}{R^2}\int_{-y_1}^{y_1}\frac{d\sigma}{d\Omega}dy, \tag{2}$$

where $d\sigma/d\Omega$= the differential-Coulomb-scattering cross section per unit solid angle and per target molecule for protons of energy E_c; y_1= the half-length of the slit; and R= the distance from collision chamber to the detector. When Eq. (2) is substituted in Eq. (1), the slit width w cancels out. Therefore, this width does not have to be known to deduce cross sections.

The differential scattering cross section was calculated from the expression

$$d\sigma/d\Omega=2\alpha/E_c^2\theta^4, \tag{3}$$

where θ= the Coulomb scattering angle which varies over the area of the slit at position x_c from 14 to 33 mrad; and α= a correction factor for electronic screening of the proton-proton interaction force. In this expression atomic units are used. The energy unit is 2 Ry, the cross section unit is a_0^2 where a_0= the Bohr radius, angles are in radians, and solid angles in steradians. The dimensionless factor α was calculated under the assumptions that the incident proton proceeded along a straight-line path through the target molecule and that the transverse momentum impulse received by the incident proton was equal to that imparted by a target proton screened by a hydrogen-atom $1s$ electronic density distribution. For the case $E_c=20$ keV, and the slit position $x_c=0.232$ in. employed in the Coulomb scattering measurement, the impact parameter was 0.1 a_0 for scatterings into the center of the slit and 0.043 a_0 for scatterings into the end of the slit. The values of α corresponding to these extremes were 0.980 and 0.999. Since the smaller scattering angles are weighted most heavily in the measurement, α was set equal to 0.980.

In the range of impact parameters corresponding to the Coulomb scattering angular range utilized, the probability of interaction with more than one of the protons within an H_2 molecule is very small since the mean nuclear distance is 1.4 a_0 or 14 times the maximum impact distance. The probability of the target molecule being oriented so that comparable scattering impulses are received from both protons of the molecule is about 10^{-3}.

The measurements of Lockwood and Helbig[14] show that at the scattering angles utilized in the present Coulomb scattering measurement, the protons have an appreciable probability of being neutralized by capturing an electron. For this reason it is important for our purposes to observe the total count of scattered particles without regard to their charge state.

In order to determine $\sigma_1(E)$, the ratio $\sigma_1(E)/\sigma_2(E)$

was first determined. Then values of $\sigma_2(E)$,determined as described above, were used to calculate $\sigma_1(E)$ from the cross-section ratio. The formulas employed to calculate this ratio were as follows:

$$\sigma_1(E)/\sigma_2(E)=[M(E)-A]/2(B-A), \quad (4)$$

$$M(E)=N_0(T_b,E)/N_0(T_a,E), \quad (5)$$

$$A=N_-(T_b,E_m)/N_-(T_a,E_m), \quad (6)$$

$$B=n_c(T_b,E_c,x_c)/n_c(T_a,E_c,x_c), \quad (7)$$

where T_b= the higher standard collision-chamber temperature; N_-= the yield of H^- ions (from reaction III) determined by a slit scan normalized to the same basis as N_0. The measurement of N_- was conducted at proton energy E_m=20 keV at which the cross section for reaction III attains a relative maximum of 10^{-17} cm^2/molecule.[17]

It should be emphasized that the quantities N_0, N_-, and n_c are differences of collision product yields at the two different collision-chamber gas pressures corresponding to the higher and lower standard gas flow rates. In general the higher flow rate collision product yields were much higher than those at the lower flow rate. Differences were taken in order that the small yield of collision products produced by proton interaction with the residual gases and at the edges of apertures S1 and S2, which were assumed to be independent of H_2 gas flow rate, would be cancelled out and would not affect the cross-section calculation.

The quantity A is assumed to be equal to the ratio of the H_2 molecule density at the two standard temperatures. This quantity was determined at three different times during the investigation and was found to fall in the range 0.065±0.004.

Quantity B is the ratio of the Coulomb scattering intensity at the two standard oven temperatures and is assumed to be equal to the ratio of the total density of protons contained within the H atoms and H_2 molecules in the target chamber at the two standard temperatures. This quantity was found to have the value 0.309±0.006 in three different determinations taken at various times during the measurement period. The fraction of H atoms contained in undissociated H_2 molecules at the higher standard temperature is easily shown to be equal to A/B=0.21. A 2.8% correction was applied to the "raw" ratio B to account for the slight H-atom beam broadening which occurred when the furnace was hot and which tended to make the Coulomb scattering intensity $n_c(T_b,E_c,x_c)$ slightly larger than it would be if there were no beam broadening due to heating.

A systematic error can arise in this kind of measurement from nonuniformity of the slit width. If the slit were slightly wider at the center portion, where the H and H^- beams were concentrated when the quantities N_0 and N_- were determined, than the average width for the broader portion of the slit effective in the n_c measurements, an error in σ_2 would result. The slit

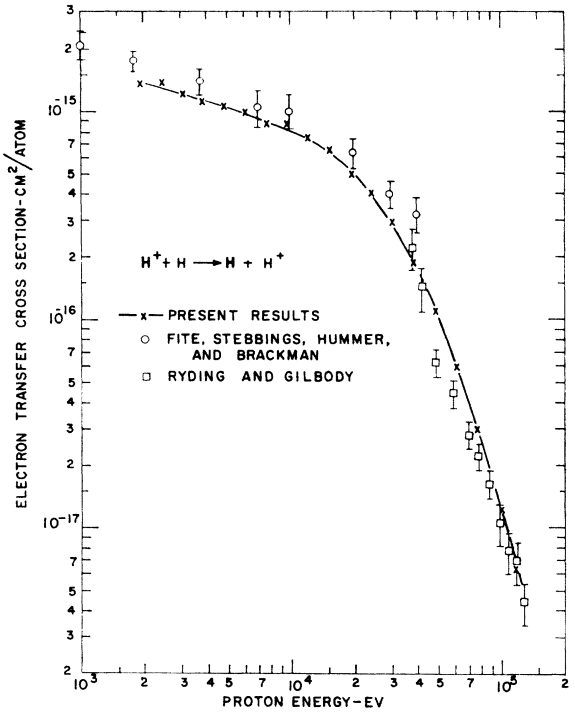

FIG. 4. Results of measurements of cross section σ_1 for reaction I. Present results are compared with data of Fite, Stebbings, Hummer, and Brackman (Ref. 10) and Ryding and Gilbody (Ref. 12).

width was examined by scanning the slit vertically along the narrow H beam and was found to be uniform to within 6%. The specific irregularities were so located as to cause an estimated error of only 1% in the σ_2 determination, however.

Another source of systematic error lies in the sensitivity of the Coulomb scattering measurements to impurities. At the chosen slit position x_c for the scattering measurements, the atomic differential cross sections for Coulomb scattering by possible impurities such as C, N, O, and W are, respectively, 12, 14, 15, and 46 times as great as for H. The use of a Ni leak to purify the H_2 gas should reduce the errors due to such impurities to less than 0.1%.

The measured values of M ranged from 0.980 at E=2 keV to 0.257 at 117.5 keV. The uncertainty in M was ±2% and the over-all experimental uncertainty in σ_1/σ_2 was ±3%. The calculated uncertainty in the final values of σ_1 is ±5%. These estimates are based on a study of the expected and observed random variations in N_0, N_-, and n_c values taken from day to day throughout the measurement period. The observed variations were accounted for by consideration of counter drive mechanism positioning irregularities, statistical fluctuations in recorded counts, and random variations in gas flow rate about the standard values during the data runs. The H^+ ion energy calibration was accurate to a fraction of 1%.

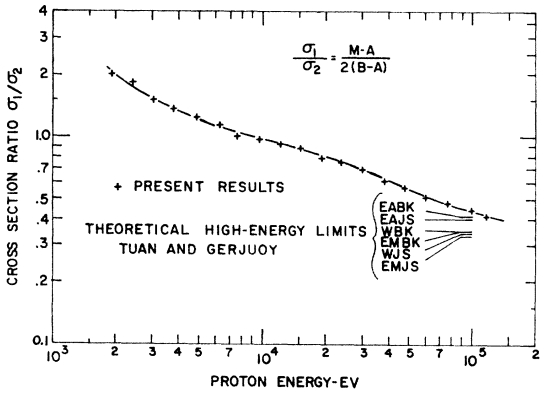

FIG. 5. Results of measurement of σ_1/σ_2 where σ_1 is the cross section for reaction I per target atom and σ_2 is the cross section for reaction II per target molecule. Theoretical high-energy limits calculated by Tuan and Gerjuoy (Ref. 21) are shown. The various theoretical limits are identified as follows: EA denotes use of atomic wave functions in the calculation, EM denotes use of molecular wave functions, W denotes use of Weinbaum wave functions, JS denotes use of Jackson and Schiff method of calculating the cross section, BK denotes the use of Brinkman and Kramer's method of calculating the cross section.

IV. RESULTS

A. Cross Section σ_1

Results obtained for the cross section σ_1 are shown in Fig. 4 together with values from earlier experiments of other workers. The results are given in numerical form in Table I.

The most probable values of σ_1 obtained by Fite and co-workers[10] are greater than the present values by 20–40% between 2 and 20 keV. Their error bars overlap the range of uncertainty of the present results only in the 4- to 20-keV energy range. At 40 keV the Fite result is greater than ours by a factor of 1.9. This disparity is not reconciled by the combined identified experimental uncertainties of the two measurements.

TABLE I. Cross sections σ_1 and σ_2 as a function of proton energy E.

E (keV)	σ_2 (10^{-16} cm^2)	σ_1 (10^{-16} cm^2)
1.92	6.8	13.3
2.41	7.5	13.6
3.04	8.1	12.1
3.82	8.3	11.1
4.8	8.7	10.5
6.05	8.8	9.85
7.62	8.9	8.8
9.6	8.9	8.6
12.1	8.2	7.5
15.2	7.5	6.5
19.2	6.7	5.0
24.1	5.5	4.1
30.4	4.3	2.97
38.2	3.06	1.86
48.0	1.97	1.10
60.5	1.18	0.60
76.2	0.63	0.30
100	0.28	0.124
117.5	0.155	0.064

The Ryding and Gilbody[12] results agree with the present data in the two ranges 38–42 keV and 80–120 keV but disagree in the intermediate region. The discrepancy in the neighborhood of 50 keV is unexplained.

The present cross-section curve is relatively smooth and does not show a sharp break in slope at ~40 keV suggested by the previous experimental data.

B. Ratio σ_1/σ_2

The results obtained for ratio σ_1/σ_2 are shown in Fig. 5. These values were obtained directly from the use of Eq. (4). The ratio varies from 1.95 at 1.92 keV to 0.41 at 117.5 keV showing very little structure except for a gradual hump in the 10–30-keV region. At the highest energy of this study, the measured ratio agrees with the highest of the theoretical high-energy limits given by Tuan and Gerjuoy.[21]

C. Cross Section σ_2

The results obtained for the cross section σ_2 of reaction II are shown in Fig. 6 together with results of several other measurements.[22–27] In the energy region 2 to 20 keV the present results are in satisfactory agreement with all other results considering the combined experimental uncertainties. Above 20 keV there is a rather large scatter of experimental values with the Ribe results lying lowest and the present results lying highest. In this range our results agree very well with those of Stier and Barnett. The vertical spread at high energies is very difficult to account for in terms of estimated errors in the cross-section values; however, a 15% discrepancy in energy-scale calibrations could reconcile all of the experimental data in the high-energy range. In the present experiments care was taken to assure that the energies were accurate to 1%.

D. Comparison of σ_1 with Theory

The present experimental results are compared with several theoretical calculations in Fig. 7. At energies greater than 25 keV, where capture into excited states is very important,[2,6,28,29] we have shown only predictions which take excited-state capture into account. At energies lower than 25 keV the theoretical predictions shown include only 1s capture except for the Wilets

[21] T. F. Tuan and E. Gerjuoy, Phys. Rev. **117**, 756 (1960).
[22] P. M. Stier and C. F. Barnett, Phys. Rev. **103**, 896 (1956).
[23] F. L. Ribe, Phys. Rev. **83**, 1217 (1951).
[24] R. Curran, T. M. Donahue, and W. H. Kasner, Phys. Rev. **114**, 490 (1959).
[25] J. B. H. Stedeford and J. B. Hasted, Proc. Roy. Soc. (London) **A227**, 466 (1955).
[26] F. Schwirzke, Z. Physik **157**, 510 (1960).
[27] I. M. Fogel, L. I. Krupnik, and B. G. Safronov, Zh. Eksperim. i Teor. Fiz. **28**, 589 (1955) [English transl.: Soviet Phys.—JETP **1**, 415 (1955)].
[28] D. R. Bates and A. Dalgarno, Proc. Phys. Soc. (London) **A66**, 972 (1953).
[29] R. F. Stebbings, R. A. Young, C. L. Oxley, and H. Ehrhardt, Phys. Rev. **138**, 1312 (1965).

and Gallaher calculation[6] which includes $1s$, $2s$, and $2p$ capture.

The Jackson and Schiff calculation, a version of the Born approximation including capture into all higher states,[30] gives cross-section values smaller than the present experimental values by 20 to 40% in the energy range 30 to 117 keV. The calculation of McElroy[2] using the Bates approximation and including capture into all excited states agrees with the present data between 25 and 55 keV but gives a cross-section value about 40% higher than the measured value at 117 keV. McCarroll's calculation[31] also based on the Bates approximation but including only $1s$ capture, agrees with the experiment at 2 keV where, according to theory, the total capture cross section includes only a small contribution from excited final states.

The calculations of Wilets and Gallaher,[6] utilizing many-term wave function expansions but not including capture into the third and higher quantum states, agree well with the present data at 2.5, 10, and 15 keV, but fall 22% below the measurement at 30 keV.

Cheshire[3,4] has conducted impulse approximation calculations of electron capture into the $1s$ state by two methods. The simpler approximation[3] agrees with the Born $1s$-state calculation of Jackson and Schiff at 95 keV but gives results 32% greater than the Born estimate at 30 keV. The Cheshire higher approximation[4] also agrees with the Born calculation at 95 keV but is a factor of 2.2 higher than the Born calculation at 30 keV.

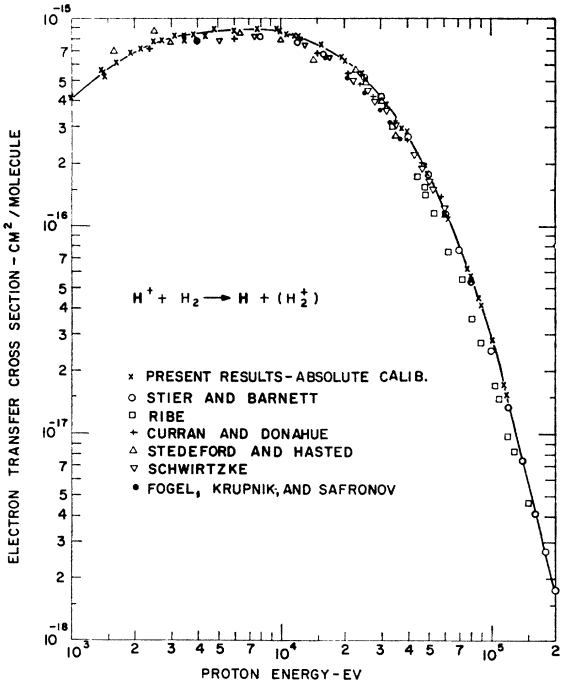

FIG. 6. Results of measurement of cross section σ_2 for reaction II. Present results based on Coulomb scattering absolute calibration are compared with results of Stier and Barnett (Ref. 22), Ribe (Ref. 23), Curran and Donahue (Ref. 24), Stedeford and Hasted (Ref. 25), Schwirzke (Ref. 26), and Fogel, Krupnik, and Safronov (Ref. 27). The curve is drawn to fit the present data at energies lower than 117.5 keV and is drawn to fit the Stier and Barnett data at energies higher than 117.5 keV.

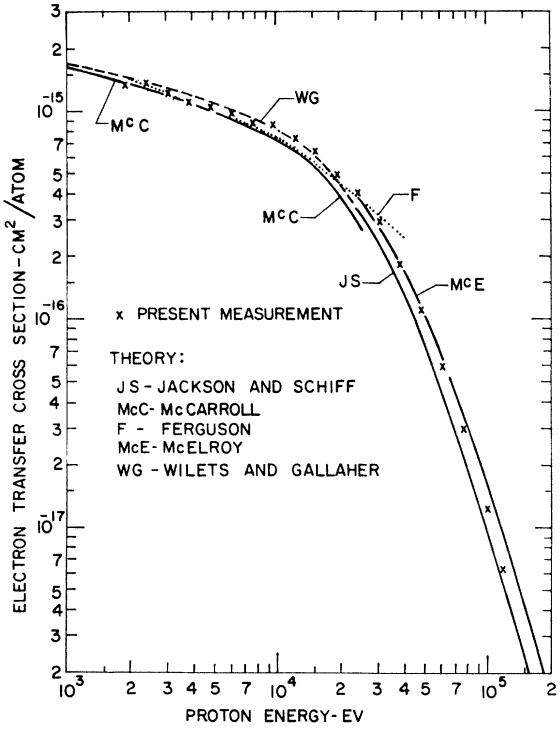

FIG. 7. Present measurement of cross section σ_1 for reaction I compared with theoretical results of Jackson and Schiff (Ref. 30), McCarroll (Ref. 31), Ferguson [Proc. Roy. Soc. (London) **A264**, 540 (1961)], McElroy (Ref. 2), and Wilets and Gallaher (Ref. 6). Comparison with other theoretical results is given in the text.

Bassel and Gerjuoy[32] have developed a theoretical treatment basically similar to that of Bates. When their theoretical result for $1s$ capture is corrected for excited-state capture by the correction factor of Jackson and Schiff[30] the final result is in excellent agreement with the present experimental data. This agreement appears fortuitous, however, in the light of the discussion given by McCarroll[31] of the Bassel-Gerjuoy cross-section formula.

A distorted-wave calculation similar to that of Bates, but retaining terms of third order in the interaction potentials, has been carried out by Grant and Shapiro.[7] Their results for capture into the $1s$ state when corrected for capture into all final states by the method they outlined lie from 40 to 60% above the present measured values in the range 25 to 100 keV.

The various calculations[8] of capture into the $1s$ state by the adiabatic theory are higher than the present experimental values by about 10% at 10 keV. The difference observed at this energy is presumably due to the

[30] J. D. Jackson and H. Schiff, Phys. Rev. **89**, 359 (1953).
[31] R. McCarroll, Proc. Roy. Soc. (London) **A264**, 547 (1961).
[32] R. H. Bassel and E. Gerjuoy, Phys. Rev. **117**, 749 (1960).

neglect of momentum transfer in the adiabatic theory. The conclusion that momentum transfer becomes important in this energy range is consistent with the theoretical results of McCarroll.[31]

A basic assumption in both the Born and impulse approximations is that the capture probability is small. This assumption is not consistent with results of McCarroll[31] which indicate for energies of about 25 keV a high capture probability in a range of impact parameters which contributes heavily to the total charge transfer cross section.

In conclusion, it appears that no existing theoretical calculation gives comprehensive agreement with the measurement over the entire energy range of this experiment, but several calculations agree over a part of the energy range.

ACKNOWLEDGMENTS

The author is greatly indebted to D. L. Allensworth for constructing the apparatus and conducting the measurements and to G. J. Lockwood for valuable advice on the construction of the collision chamber. Thanks are also due to T. A. Green and J. M. Peek for calling the author's attention to a number of relevant theoretical papers and for numerous discussions concerning the various theoretical methods.

PHYSICAL REVIEW VOLUME 148, NUMBER 1 5 AUGUST 1966

Cross Section for Energy Transfer between Two Moving Particles*

E. GERJUOY
Department of Physics and Space Research Coordination Center, University of Pittsburgh, Pittsburgh, Pennsylvania
(Received 4 January 1966)

The classical cross section $\sigma_{\Delta E}$, for producing a specified energy transfer ΔE in the collision of two particles 1,2 having arbitrary masses and velocities $\mathbf{v}_1,\mathbf{v}_2$ in the laboratory system, is derived. The effective average (for fixed speeds v_1,v_2) of $\sigma_{\Delta E}$ over all directions of the particle velocities $\mathbf{v}_1$ and/or $\mathbf{v}_2$ is then computed. These results are required in the classical calculations of atomic-collision cross sections via the procedures recently proposed by Gryzinski. The method will yield the average of any function $F(v,V,\cos\bar{\theta})$ over all directions of the particle velocities, where $\mathbf{v}=\mathbf{v}_1-\mathbf{v}_2$, $\mathbf{V}$ is the velocity of the center of mass, and $\bar{\theta}$ is the angle between $\mathbf{v}$ and $\mathbf{V}$.

I. INTRODUCTION

RECENTLY, Gryzinski has published three papers[1–3] detailing his procedures for performing classical (nonquantum) calculations of atomic-collision cross sections. The utility of these procedures in electron-atom and electron-molecule collisions has been examined by Bauer and Bartky.[4] For such collisions, one requires the cross section $\sigma_{\Delta E}(\mathbf{v}_1,\mathbf{v}_2)$ for producing an energy transfer ΔE in the collision of two electrons moving with arbitrary velocities $\mathbf{v}_1$, $\mathbf{v}_2$ in the laboratory system. There also is required $\sigma_{\Delta E}{}^{\text{eff}}(v_1,v_2)$ the effective average of $\sigma_{\Delta E}(\mathbf{v}_1,\mathbf{v}_2)$ over all orientations of $\mathbf{v}_1$ and/or $\mathbf{v}_2$ for fixed speeds v_1, v_2. Gryzinski has derived expressions for these quantities, but use of these formulas is complicated by an extremely awkward notation; moreover Gryzinski's expressions involve some subsidiary approximations. For these reasons, Stabler[5] has rederived—and obtained in much simpler form—the exact expressions for $\sigma_{\Delta E}$ and $\sigma_{\Delta E}{}^{\text{eff}}$ in electron-electron collisions. Similar expressions have been obtained by Ochkur and Petrun'kin.[6] However, these authors[5,6] have rederived $\sigma_{\Delta E}$ only for electron-electron collisions, i.e., for colliding particles of equal mass, whereas for calculations of, e.g., ion-atom collisions by Gryzinski's procedures, one requires $\sigma_{\Delta E}$ and $\sigma_{\Delta E}{}^{\text{eff}}$ for collisions of unequally massive charged particles.

This paper derives the required exact formulas for $\sigma_{\Delta E}$ and $\sigma_{\Delta E}{}^{\text{eff}}$ in the unequal-mass case. Application of these formulas to examination of the utility of Gryzinski's procedures in charge-transfer reactions is under way (in cooperation with Hsiang Tai and Jean Welker). This paper obtains the final formula for $\sigma_{\Delta E}{}^{\text{eff}}(v_1,v_2)$ in only one case, namely, Coulomb collisions; it will be clear, however, that the method of performing the average over all orientations is applicable to arbitrary interactions, as well as to the averages of quantities other than $\sigma_{\Delta E}(\mathbf{v}_1,\mathbf{v}_2)$.

II. CALCULATION OF $\sigma_{\Delta E}$

I consider a collision between particles 1 and 2, whose initial velocities in the laboratory system are $\mathbf{v}_1=v_1\mathbf{n}_1$

* Supported by the National Aeronautics and Space Administration under Contract NGR-39-011-35 and Research Grant N-s-6-416.

[1] M. Gryzinski, Phys. Rev. 138, A305 (1965).
[2] M. Gryzinski, Phys. Rev. 138, A322 (1965).
[3] M. Gryzinski, Phys. Rev. 138, A336 (1965).
[4] E. Bauer and C. D. Bartky, J. Chem. Phys. 43, 2466 (1965).
[5] R. C. Stabler, Phys. Rev. 133, A1268 (1964).
[6] V. I. Ochkur and A. M. Petrun'kin, Opt. i Spectroskopiya 14, 457 (1963) [English transl.: Opt. Spectry. (USSR) 14, 245 (1963)].